Biofilm 8 (2024) 100225

Contents lists available at ScienceDirect

Biofilm

journal homepage: www.sciencedirect.com/journal/biofilm

Salmonella biofilm formation diminishes bacterial proliferation in the *C. elegans* intestine

Ines Thiers, Maries Lissens, Hanne Langie, Bram Lories [1], Hans Steenackers [1,*]

Centre of Microbial and Plant Genetics (CMPG), Department of Microbial and Molecular Systems, KU Leuven, Leuven, Kasteelpark Arenberg 20, 3001, Belgium

ARTICLE INFO

Keywords:
Salmonella
Biofilm
Gut colonization
C. elegans
Virulence

ABSTRACT

Non-typhoidal *Salmonella* serovars are a significant global cause of foodborne infections, owing their transmission success to the formation of biofilms. While the role of these biofilms in *Salmonella*'s persistence outside the host is well understood, their significance during infection remains elusive. In this study, we investigated the impact of *Salmonella* biofilm formation on host colonization and virulence using the nematode model *Caenorhabditis elegans*. This infection model enables us to isolate the effect of biofilm formation on gut colonization and proliferation, as no gut microbiome is present and *Salmonella* cannot invade the intestinal tissue of the nematode. We show that a biofilm-deficient Δ*csgD* mutant enhances gut proliferation compared to the wild-type strain, while the pathogen's virulence, the host's immune signaling pathways, and host survival remain unaffected. Hence, our work suggests that biofilm formation does not significantly contribute to *Salmonella* infection in *C. elegans*. However, complementary assays in higher-order *in vivo* models are required to further characterize the role of biofilm formation during infection and to take into account the impact of biofilm formation on competition with gut microbiome and epithelial invasion.

1. Introduction

Non-typhoidal *Salmonella* (NTS) infections remain a significant public health concern, affecting over 95 million individuals annually and contributing to approximately 3 million disability-adjusted life years (DALYs) worldwide [1]. The success of this enteropathogen stems from its ability to alternate between host and non-host environments [2]. To shield themselves from the inhospitable external environment, NTS serovars aggregate to one another and embed themselves into a self-produced extracellular matrix, forming so-called biofilms [3,4]. The composition of the biofilm matrix varies greatly depending on the environmental conditions, but is generally characterized by the presence of water, exopolysaccharides, proteinaceous compounds, and eDNA. The vast majority of these matrix components are under control of the major biofilm regulator CsgD. Upon *csgD* expression, EPS production is activated and a mature biofilm can be formed [3,5]. Although the role of CsgD has mainly been studied outside the host, recent work supports that *csgD* is also expressed inside the intestinal tract [6,7]. Even more, curli fimbriae, functional bacterial amyloids known to play an important role in *Salmonella* biofilms, have been detected inside the cecum and colon of orally infected mice [6]. While additional proof of biofilm formation *in vivo* is being collected, profound insight into its role during pathogenesis is missing.

In order to unambiguously determine the contribution of biofilm formation in the host, effects on distinct aspects of the infection process, such as invasion, colonization, and immune activation, need to be considered. While the currently available *in vitro* models lack the required complexity to fully capture these interactions [8,9], commonly used *in vivo* systems, such as the murine model, present challenges in distinguishing specific effects due to their inherent complexity [10]. The *Caenorhabditis elegans* infection model offers an excellent compromise. This free-living, bacterivorous roundworm is one of the best-studied laboratory organisms in life sciences due to its transparency, rapid reproduction, and ease of manipulation. The presence of evolutionarily-conserved signaling pathways and the possibility to tightly control the intestinal microbiome enhances the utility of *C. elegans* as an infectious disease model [11]. Notably, *Salmonella* has been proven to effectively colonize the *C. elegans* gut, causing persistent infection[12–14]. However, *Salmonella* is unable to invade the nematode's epithelial cells, allowing to specifically investigate the

* Corresponding author.
E-mail addresses: ines.thiers@kuleuven.be (I. Thiers), bram.lories@kuleuven.be (B. Lories), hans.steenackers@kuleuven.be (H. Steenackers).
[1] last co-authors.

https://doi.org/10.1016/j.bioflm.2024.100225
Received 27 June 2024; Received in revised form 11 September 2024; Accepted 27 September 2024
Available online 27 September 2024

contribution of biofilm formation on gut colonization and proliferation [12].

Desai et al. (2019) confirmed *Salmonella's* capacity to form sessile aggregates within the nematode's intestine. Interestingly, they observed that the non-aggregating *ssrB*-null strain actively downregulated crucial innate immune pathways, leading to a significant reduction in host survival [14]. SsrB, a component of the SsrA/SsrB two-component regulatory system, acts as a dual transcriptional regulator, activating both *csgD* and *Salmonella* pathogenicity island 2 (SPI-2) and downregulating *Salmonella* pathogenicity island 1 (SPI-1) [15–17]. This multifaceted nature of SsrB complicates the direct attribution of the effects observed by Desai et al. to cell aggregation. Consequently, in the present study, the more downstream Δ*csgD* deletion mutant was used to more specifically assess the impact of biofilm formation. We show that a biofilm-deficient strain proliferates within the *C. elegans'* intestine to a higher extent than the wild-type strain, without affecting virulence. The absence of biofilm formation did not impact SPI-1 expression or functionality, nor did it influence nematode mortality. Correspondingly, no alterations were observed in the activation of host's innate immune pathways. Therefore, our work suggests that *Salmonella* biofilms do not confer an advantage during infection in the *C. elegans* model.

2. Results

2.1. Biofilm formation diminishes intestinal proliferation

To determine the impact of biofilm formation on the establishment of *Salmonella* infection, fourth-stage *C. elegans* larvae (L4) were infected with either wild-type *S.* Typhimurium or the isogenic biofilm deficient-mutant Δ*csgD*. Hereto, worms were fed on lawns of the corresponding *Salmonella* strain for 24 h. After the infection period, worms were washed and homogenized in order to recover viable bacterial cells from the intestine (Fig. 1A). It was observed that both the wild-type and mutant strain colonized the *C. elegans* intestine to a similar extent, reaching luminal densities of 10^3 CFU/worm (Fig. 1B). Given the continuous feeding of *Salmonella* to the nematodes, comparable initial colonization levels were anticipated. As indicated by Desai et al. (2019), *Salmonella* biofilm formation is more likely to play a role in bacterial persistence [14]. Therefore, the infection profile of wild type and Δ*csgD*-subjected nematodes were compared over time. Hereto, worms were transferred to OP50 plates after 1 day of *Salmonella* exposure, and bacterial accumulation was measured at day 1, 2, and 3 post-infection (dpi). To differentiate between the effects of initial colonization and subsequent accumulation, the latter will be referred to as proliferation. As illustrated in Fig. 1B, overall cell numbers dropped equally for the wild-type and mutant strain at 1 dpi. From 2 dpi onward, the Δ*csgD* strain proliferated substantially, achieving cell counts between 10^3-10^4 CFU/worm. In contrast, the wild-type cells exhibited lower counts at 2 dpi compared to 1 dpi, averaging below 10^3 CFU/worm. Although the wild-type cells further accumulated at 3 dpi, they failed to reach levels comparable to the mutant strain, showing significant differences at 2 and 3 dpi.

2.2. Enhanced persistence in biofilm-deficient strain is not associated with SPI-1 expression

Aggregated cells have generally been associated with a reduced activity of SPI-1 and, consequently, a decreased virulence compared to their planktonic counterparts [21,22,25]. The observed difference in bacterial proliferation within the nematode gut between the wild type and the Δ*csgD* mutant in the current study could thus be due to an altered activity of virulence factors encoded on SPI-1. In order to elucidate the involvement of SPI-1 activation, we determined the gut colonization and proliferation of Δ*hilA* and Δ*hilA*Δ*csgD* deletion strains. HilA is the central regulator of the SPI-1 virulence pathway, stimulating expression of SPI-1-encoded genes [27,28]. Deletion of *hilA* has previously shown to significantly reduce SPI-1 activity, resulting in decreased virulence in both nematodes and mice [13,23].

As shown in Fig. 2A, the bacterial load of both the Δ*hilA* and Δ*hilA*Δ*csgD* mutants consistently exceeded the wild-type level, displaying trends comparable to the Δ*csgD* mutant. Consequently, deleting *hilA* in a Δ*csgD* background did not restore the wild-type phenotype. On the contrary, the absence of *hilA* seemed to have a similar effect on proliferation as the absence of *csgD*, suggesting an direct or indirect positive relation between *csgD* and *hilA*. Therefore, *hilA* expression was assessed using flow cytometry in both the wild-*type* and *csgD*-deletion strain after 24 h in nematodes. The bimodal expression patterns observed in Fig. 2B coincide with previous observations showing bistable expression of SPI-1 in physiologically relevant conditions [29–31]. However, no discernible differences in *hilA* expression were identified when comparing the wild-type and Δ*csgD* strain, rejecting a direct regulatory link between *hilA* and *csgD* in this set-up. Despite the lack of transcriptional changes, the efficacy of the SPI-1 encoded effectors could still be affected. Specifically, as the SPI-1 effector proteins are injected in the host tissue via a type three secretion system that requires epithelial adherence [32], the absence of biofilm formation could impede epithelial attachment and thus also inhibit SPI-1 effector secretion and functionality. Therefore, downstream effects of SPI-1, such as immune signaling and nematode killing, were investigated.

2.3. Matrix components do not interfere with host responses

In mammalian infections, it is widely recognized that SPI-1 effectors activate Rho-family GTPases, the mitogen-activated protein kinase

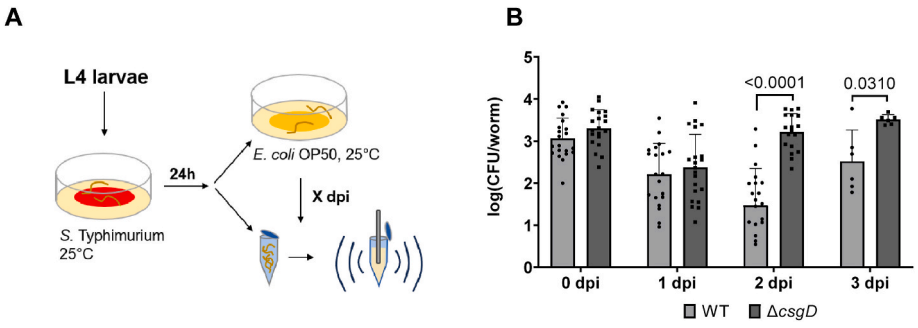

Fig. 1. *Salmonella* biofilm formation diminishes intestinal proliferation in *C. elegans*. Fourth-stage larvae were infected with either the ATCC14028 wild-type (WT) or the isogenic Δ*csgD* strain. After 24 h of *Salmonella* exposure, worms were transferred to OP50 plates and infection was followed several days post-infection (dpi). **(A)** Schematic of the experimental set-up. Synchronized L4 larvae were exposed to *S.* Typhimurium for 24 h, after which they were transferred to OP50 feeding plates. After *Salmonella* exposure and at specific dpi, nematodes were pooled and homogenized for further analysis. **(B)** The wild-type strain proliferates to significantly lower luminal densities than the Δ*csgD* strain in the worm's gut. P values are derived from mixed model analysis. Error bars show the mean ± sd ($n \geq 6$ with five worms per condition in each replicate).

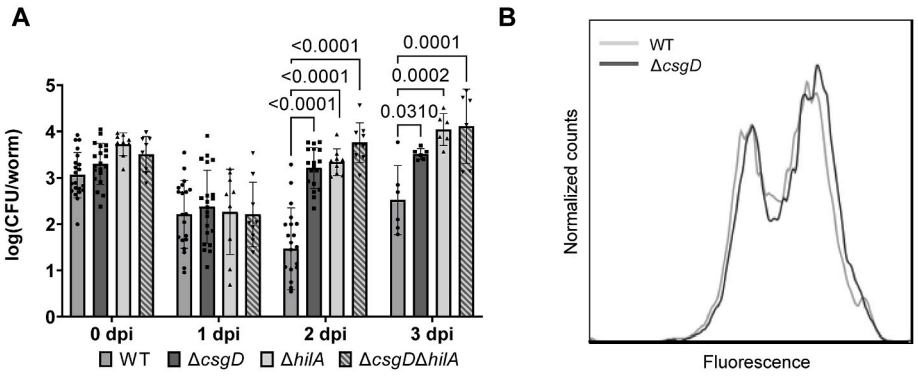

Fig. 2. Relation between *hilA* and *csgD* during *Salmonella* infection in *C. elegans*. Fourth-stage larvae were infected with either the ATCC14028 wild-type (WT) or the isogenic Δ*csgD,* Δ*hilA,* and Δ*csgD*Δ*hilA* strains. After 24 h of *Salmonella* exposure, worms were transferred to OP50 plates and infection was followed several days post-infection (dpi). **(A)** Δ*hilA* and Δ*csgD*Δ*hilA* strains proliferate to similar luminal densities as the Δ*csgD* strain in the *C. elegans* gut. P values are derived from mixed model analysis. Error bars show the mean ± sd ($n \geq 6$ with five worms per condition in each replicate). **(B)** Flow cytometric profile indicates no difference in *hilA* expression between genomically-labelled wild-type and Δ*csgD Salmonella* cells after 24 h of infection in *C elegans.* For each condition, a minimum of 1000 *Salmonella* cells were analyzed. The average of three replicates is shown (with approximately 100 worms per condition in each replicate). See also Figure S1.

(MAPK), and nuclear factor- κβ (NF-κβ) signaling pathways, leading to the production of proinflammatory cytokines[33–35]. Although nematodes lack the NF-κβ pathway, they possess a conserved p38 MAPK pathway, which plays an important role in pathogen resistance [36,37]. Accordingly, SPI-1 effectors impact p38 MAPK signaling upon infection in nematodes [14]. Next to MAPK signaling, SPI-1 also affects nematode killing, as evidenced by the increased host survival and enhanced bacterial proliferation upon *hilA* deletion [13]. Consequently, any potential reduction in SPI-1 functionality in the *csgD*-deficient strain due to a reduced adhesion to the epithelial cells could alter host responses, and concomitantly bacterial proliferation. Alternatively, matrix components themselves can influence immune signaling, as *Salmonella* amyloid curli were shown to trigger inflammatory responses in mice [6]. Therefore, we investigated the interplay between CsgD, HilA, and the immune system of the nematode.

Considering that the p38 MAPK pathway plays an essential role in the intestinal immunity of *C. elegans* [37–40], we determined the impact of the MAPK pathway on the gut colonization of the wild-type and mutant strains. Hereto, nematodes with a loss-of-function mutation in the *sek-1* gene, encoding an essential MAPK kinase [41], were infected as described above. Surprisingly, following 24h of *Salmonella* exposure and at 1 and 2 dpi, most strains showed lower bacterial loads compared to infection in immunocompetent nematodes (Fig. 3A). Given the typically higher susceptibility of MAPK-compromised nematodes to bacterial infection, heightened colonization and proliferation levels were expected[38,42–44]. However, as *C. elegans*' defense response can change depending on temperature fluctuations and the diet type, these discrepancies presumably result from nutrient batch variability and temperature variation [45]. When comparing colonization between wild-type and deletion mutants within immunocompromised nematodes, only the Δ*csgD*Δ*hilA* double mutant proliferated to significantly higher densities than the wild type at 2 dpi. However, from 3 dpi onward, all mutant strains exhibited significantly higher cell counts than the wild type, resembling the infection dynamics in immune-competent nematodes. Consequently, the increased bacterial loads of the mutant strains do not (solely) seem to result from altered MAPK activation. Accordingly, this assay did not allow us to understand the effect of biofilm formation on SPI-1 efficacy.

While the MAPK pathway serves as the primary intestinal defense mechanism, other signaling routes may also be involved. Notably, mutations in the daf/insulin-like growth factor (IGF) pathway, traditionally associated with longevity and stress resistance[46–48], have been connected to intestinal pathogen resistance [49–51]. Additionally, the growth factor-β signaling (TGF-β) pathway has recently been suggested to play a role in intestinal bacterial load regulation [52]. To directly assess the impact of biofilm formation and SPI-1 on these defense mechanisms, expression levels of *daf-16* (daf/IGF pathway), *lys-7* (daf/IGF pathway), and *sma-3* (TGF-β pathway), together with levels of *sek-1,* were measured at 2 dpi by means of qPCR. Relative expression levels of the wild type and Δ*csgD* mutant were similar for all analyzed genes, suggesting that biofilm formation does not significantly affect the immune response (Fig. 3B). Conversely, nematodes infected with the *hilA*-deficient strain displayed lower activation across all genes, with the exception of *lys-7*. Nevertheless, no significant differences in log fold change between Δ*hilA*-infected and wild type and Δ*csgD*-infected worms were detected. The similar expression levels of the wild type and *csgD*-deletion mutant suggest that biofilm formation does not impact immune signaling, neither directly, nor indirectly by affecting SPI-1 functionality. Infection with the Δ*csgD* mutant also resulted in a similar killing profile of *C. elegans* as the wild type, whereas deletion of *hilA* significantly increased host survival (Fig. 3C), further confirming that the lack of biofilm formation does not impede SPI-1 functionality.

To corroborate our findings, nematodes were subjected to mixed lawns of wild-type and *csgD*-deficient *Salmonella*. In this scenario, modulation of immune pathways by one strain was anticipated to also impact the other strain. CFU counting confirmed the 50:50 ratio on the feeding plates before and after infection (Figure S2). In the worm, the Δ*csgD* mutant significantly outperformed the wild-type strain, reaching significantly higher levels at 2 dpi (Fig. 3D). This further supports that the colonization difference between the wild type and Δ*csgD* mutant cannot be attributed to host responses, especially given that confocal microscopy showed colocalization of both strains throughout the nematode's gastrointestinal tract (Fig. 3E).

3. Discussion

The use of simple and easily manipulated model organisms in studying pathogen-host interactions originates from pioneering studies with the predatory amoeba *Dictyostelium discoideum,* and remains relevant through investigations involving the soil-dwelling nematode *C. elegans* [12,53]. The bacterivorous nature of *C. elegans* facilitates bacterial infection and precise control of microbiome composition. Moreover, the nematode's evolutionarily conserved innate immune pathways provide relevant insights into host manipulation by pathogens. Recently, *C. elegans* has emerged as a valuable asset in intestinal biofilm research. Microbial biofilm formation within the nematode's gut has shown to impact bacterial proliferation and host lifespan, with outcomes favoring or opposing the nematode depending on the pathogenicity of the involved microbe[14,54–57]. Here, we demonstrate that biofilm formation by *Salmonella* Typhimurium in *C. elegans* impairs

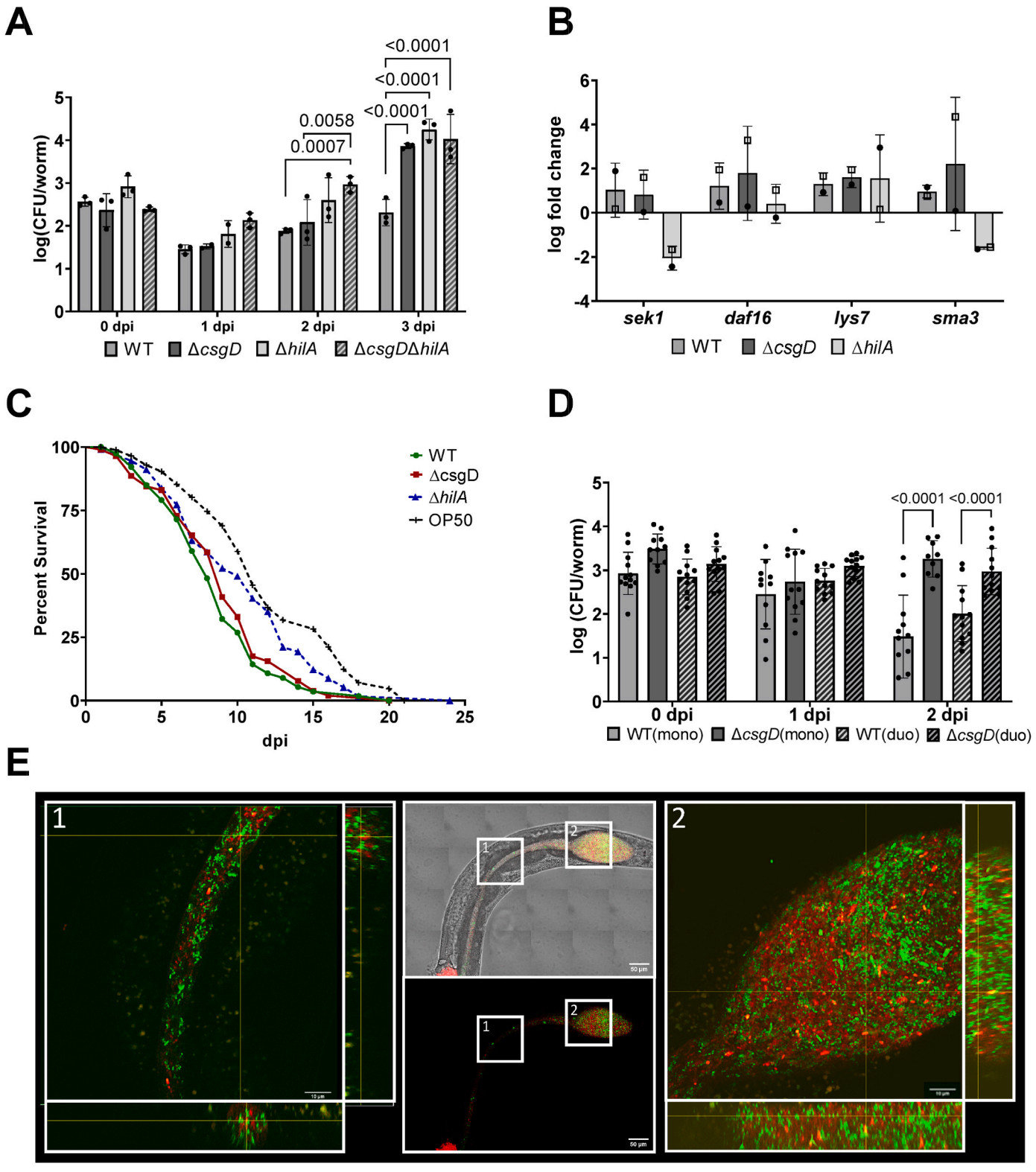

(caption on next page)

Fig. 3. *Salmonella* biofilm components do not seem to induce immune signaling pathways in *C. elegans*. Fourth-stage larvae were infected with either the ATCC14028 wild-type (WT) or the isogenic Δ*csgD,* Δ*hilA,* and Δ*csgD*Δ*hilA* strains. After 24 h of *Salmonella* exposure, worms were transferred to OP50 plates and infection was followed several days post-infection (dpi). **(A)** Δ*csgD,* Δ*hilA* and Δ*csgD*Δ*hilA* strains proliferate to significantly higher luminal densities than the wild-type strain in Δ*sek-1(km4)* mutant worms. P values are derived from mixed model analysis. Error bars show the mean ± sd (n = 3 with five worms per condition in each replicate). **(B)** qPCR analysis shows no significant difference in upregulation of immune signaling pathways in *C. elegans* after infection with different *Salmonella* strains. Error bars show the mean ± sd. (n = 2 with approximately 500 worms per condition in each replicate. Filled bullets represent data from the first replicate, whereas open squares represent data from the second replicate). **(C)** Worms infected with wild-type *Salmonella* die equally fast as worms infected with the Δ*csgD* mutant. Both die significantly faster than OP50-subjected control worms, as indicated by log-rank tests with Bonferroni multiple comparisons correction ($P_{WT\text{-}\Delta csgD} = 1$, $P_{WT\text{-}OP50} = 0.0002$, $P_{\Delta csgD\text{-}OP50} = 0.0005$, $P_{WT\text{-}\Delta hilA} = 0.0808$, $P_{\Delta csgD\text{–}\Delta hilA} = 0.2278$, $P_{\Delta hilA\text{-}OP50} = 0.2459$) (n = 2 with approximately 50 worms per condition in each replicate). **(D)** The Δ*csgD* mutant proliferates to significantly higher luminal densities than the wild-type strain in *C. elegans,* both in mono- and in coculture. P values are derived from mixed model analysis. Error bars show the mean ± sd (n ≥ 9 with five worms per condition in each replicate). **(E)** Confocal images indicate colocalization of the wild-type (green) and Δ*csgD* (red) strain within Δ*sek-1(km4)* mutant worms at 3 dpi. Middle images show an overview (scale bars indicate 50 μm), and left and right images show zoomed-in orthogonal micrographs (scale bars indicate 10 μm). Images were taken with a Zeiss LSM 880 confocal microscope (63× objective) and analyzed with the associated Zen Blue and Fiji software. Imaging was replicated three times with at least five worms per condition in each replicate. (For interpretation of the references to colour in this figure legend, the reader is referred to the Web version of this article.)

intestinal proliferation during early stages of infection, while leaving host signaling and survival unaffected.

In contrast to the findings of Desai et al. (2019), which associated *Salmonella* biofilm formation with prolonged host survival, our study reveals no disparity in nematode lifespan after exposure to a wild-type or Δ*csgD* mutant strain [14]. Even more, biofilm formation diminished intestinal proliferation, with the mutant reaching significantly higher cell counts at 2 and 3 dpi. Considering that Desai et al. employed the more upstream *ssrB*-null strain, their observed reduction in lifespan may not result solely from the lack of aggregate formation [14]. Importantly, SsrB acts as a dual regulator, silencing SPI-1 expression while inducing SPI-2 and *csgD* activation[15–17]. In mammalian hosts, this regulatory switch aids in transitioning from the extracellular to the intracellular environment upon host cell invasion. Considering that *S.* Typhimurium is uncapable of invading intestinal epithelial cells in healthy metazoan hosts, the role of SPI-1 and SPI-2 effectors is less straightforward in *C. elegans*. Although their exact contribution to virulence is not fully understood yet, both SPI-1 and SPI-2 deletion mutants have shown to extend the nematode's lifespan [13,23]. Also in this study, a *hilA*-deletion mutant appeared less virulent than the wild-type strain, with infected nematodes showing enhanced survival and lower immune stimulation.

Considering that biofilm formation and virulence have been linked in literature, we looked into the effects of *csgD* deletion on SPI-1 activity. Traditionally, bacterial biofilms in general have been associated with chronic infections, characterized by high levels of proliferation and impaired virulence[18–20]. Although supporting evidence in literature is scarce, an inverse relationship between biofilm formation and virulence has also been proposed in the context of NTS infections specifically [25]. For instance, comparative analyses between planktonic and aggregated cells revealed a decreased expression of virulence genes located on SPI-1 in the latter [21,22]. Additionally, during competition experiments in mice, non-aggregated cells consistently outperformed their aggregated counterparts, displaying a strong virulence advantage [21]. However, in the current study, deletion of *hilA* in the Δ*csgD* background did not restore the wild-type phenotype. Even more, deletion of *hilA* in a wild-type background seemed to have similar effects on bacterial proliferation as deletion of *csgD,* suggesting a positive rather than a negative link. Nonetheless, verification using flow cytometry could not confirm this positive association, given that the biofilm mutant exhibited a similar *hilA* expression profile as the wild-type strain.

Not only *hilA* expression appeared unmodified in the absence of biofilm formation, also host responses were not significantly affected. RNA analysis revealed no significant difference in immune activation between the wild-type and biofilm-deficient strain, nor did infection in immune-deficient nematodes change the proliferation dynamics. These findings seem to be *Salmonella*-specific, considering that bacterial biofilms have already been shown to interact with nematode signaling. For example, biofilm formation by *Staphylococcus* enhanced pathogenesis in immunocompetent worms, but not in MAPK-deficient nematodes [54, 58]. Also EPS produced by commensals have been reported to interact with the nematode's signaling pathways, as exposure to *B. subtilis, Lactobacillus rhamnosus,* and *Pseudomonas fluorescens* biofilms resulted in oxidative stress-mediated resistance to pathogens [55,57]. The effect of matrix components on the host thus seems to vary significantly depending on the species.

Remarkably, luminal colonization by *Salmonella* is not positively correlated with virulence in *C. elegans*. *hilA* knock-out mutants reached significantly higher luminal densities than the wild-type strain, albeit increasing nematode lifespan. Comparable trends related to *hilA* were reported by Portal-Celhay and Blaser (2012), who performed colonization and lifespan assays using a Δ*spi-1*Δ*spi-2* strain. Concomitant with the higher intestinal load, they observed enhanced nematode survival after infection with the *spi-1* and *spi-2* deficient strain [13]. Presumably, SPI-1 effectors damage the epithelial layer, subsequently not only harming the host, but also hampering effective colonization by *Salmonella*. This phenomenon was previously reported for *Pseudomonas aeruginosa,* where *Pseudomonas* either slowly kills the nematodes by accumulating in the intestine, or rapidly by excreting highly toxic compounds [59]. However, this hypothesis does not apply to infection with the Δ*csgD* strain. Here, augmented colonization was not associated with lower nematode survival, possibly due to unaltered SPI-1 expression. The lower bacterial load of the wild type compared to the *csgD* deletion mutant could be explained by the cost associated with EPS production. Indeed, we previously showed that EPS production by *Salmonella* is costly [60]. Also studies on other bacteria, including *Bacillus subtilis, Vibrio Cholerae* and *Pseudomonas aeruginosa* confirmed the costly production of EPS using a combination of competition assays, single-gene expression analyses and metabolic modeling[61–64]. However, the cost of matrix production is known to vary depending on the environmental conditions, making it challenging to formulate specific claims about its impact in the intestinal environment [65].

In summary, *Salmonella* biofilm formation does not appear to contribute to infection establishment in *C.elegans*. Matrix production had no discernible effect on virulence, and even impaired intestinal colonization in the worm. These findings should be interpreted with caution and not be generalized as infection in *C. elegans* differs significantly from infection in mammals. Notably, C. *elegans* infections do not involve epithelial cell invasion and a microbiome is absent during growth under conventional laboratory conditions. Where this allowed us to specifically investigate the role of EPS components on epithelial attachment and luminal proliferation, this leaves out their contribution to competition with the microbiome and intracellular replication. Additionally, considering that *C.* elegans is grown at temperatures below 25 °C and that the activity of CsgD is temperature-dependent, the regulation of *Salmonella* biofilm and/or virulence factors in the worm can differ from regulation in mammals [66]. Complementary assays in higher order *in vivo* models will consequently be required to further characterize the role of biofilm formation in gut colonization and infection.

4. Material and methods

4.1. Caenorhabditis elegans strains and growth conditions

Two distinct *C. elegans* strains were utilized in this study, namely strain AU37 Δ*glp-4(bn2)* and strain AU37 Δ*glp-4(bn2)*Δ*sek-1(km4)*. The former was kindly provided by Bart Braeckman (Ghent University), whereas the latter was obtained from the *Caenorhabditis* Genetic Center. All nematodes were maintained at a constant temperature of 16 °C on Nematode Growth Medium (NGM) plates seeded with *Escherichia coli* OP50 and supplemented with 100 μg/mL ampicillin following standard maintenance procedures [67].

4.2. Bacterial strains, plasmids, and growth conditions

Experiments were conducted using wild-type *Salmonella enterica,* subsp. *enterica* serovar Typhimurium ATCC14028 [68] and isogenic deletion mutants Δ*csgD*, Δ*hilA,* and Δ*csgD*Δ*hilA*. Mutants originated from the McClelland mutant library and were transferred to a clean genetic background using P22 phage transduction [69,70]. Primers used to verify the deletions are shown in Table S1. In order to distinguish between the different mutants, the *Salmonella* strains harbored plasmids encoding either a green (wild type and Δ*hilA*) or a red (Δ*csgD* and Δ*csgD*Δ*hilA*) fluorescent protein (pFPV25.1; gfpmut3; Ap^R and pFPV25.1; dsred; Ap^R, respectively) [71]. For flow cytometric analyses, wild-type and Δ*csgD Salmonella* were genomically labelled with mRFP1 via scarless genome editing [72] (Table S1). *E. coli* OP50 served as a food strain for the nematodes and was transformed with the pUC18.1 *sacB sacR* plasmid (Ap^R) in order to differentiate between *Salmonella* and OP50 during colonization assays [73].

All bacterial strains were cultivated in Luria-Bertani (LB) medium supplemented with ampicillin (100 μg/mL) at 37 °C in shaking conditions. Nematode infection and feeding plates were prepared using standard conditions: 150 μL of normalized *Salmonella* or *E. coli* OP50 culture were spread onto NGM + Ap agar plates and incubated overnight at 37 °C, creating lawns of bacteria for nematodes to feed on.

4.3. Nematode age synchronization

To ensure uniform developmental stages, nematodes were age-synchronized using a bleaching procedure [67]. Briefly, nematodes were washed off NGM plates with M9 buffer and subjected to a 3 mL bleaching solution (1/3 5 M NaOH, 2/3 bleach). Following repeated washing steps, the eggs were allowed to recover overnight at 16 °C with gentle rotation. Subsequently, the L1 larvae were spotted onto standard feeding plates and incubated at 25 °C for 48 h in order to reach the L4 stage.

4.4. Quantification of bacterial colonization in C. elegans

Intestinal bacteria were quantified as described previously [74]. In short, synchronized L4 larvae were spotted onto NGM plates seeded with normalized *Salmonella* culture at 25 °C. Following a 24-h infection period, the nematodes were transferred to standard feeding plates and maintained at 25 °C. At the designated time points, 15 worms per plate were collected using a platinum wire and transferred to M9 buffer supplemented with 25 mM levamisole (M9+Lev). Levamisole was employed to induce paralysis and inhibit pharyngeal pumping. Subsequently, the worms were washed twice in M9+Lev and then twice more in M9+Lev containing 100 μg/mL gentamycin. After the final washing step in M9+Lev + gentamycin, the nematodes were incubated in this antibiotic solution for 1 h at room temperature in order to kill remaining bacterial cells attached to the outside of the worm. Following two additional washing steps with M9+Lev, the nematodes were pooled in groups of 5 and mechanically disrupted using the Kimble® pestles on a motor (Sigma-Aldrich). The number of *Salmonella* cells within the worm's intestine could in turn be determined by plating out the lysates and performing colony-forming unit counts.

4.5. C. elegans lifespan analysis

Lifespan analysis was performed as previously described [74]. Shortly, approximately 50 L4 larvae were infected with *Salmonella* for 24 h and subsequently transferred to standard feeding plates at 25 °C. Survival was monitored daily with worms non-responsive to touch considered to be death. Nematodes that crawled into or off the ager, and nematodes that died due to a protruding vulva were excluded from analysis [75].

4.6. Immune response monitoring

At 3 dpi, around 500 worms were collected and subjected to a series of washing steps in M9 buffer. After the final washing step, worms were snap-frozen in liquid nitrogen and stored at - 80 °C or used immediately for subsequent analysis steps. Worms were mechanically lysed and total RNA was extracted using the RNAeasy® Plus Mini Kit (Qiagen GmbH) according to the manufacturer's protocol. Following RNA isolation, the samples were treated with DNAseI (Qiagen GmbH) for 15 min at room temperature to eliminate genomic DNA. Removal of gDNA was confirmed with PCR, while RNA integrity and concentration were verified using the Nanodrop® ND-1000 Spectrophotometer (Thermo Scientific).

Total RNA was converted into cDNA using M-Mulv reverse transcriptase (Bioké), following the manufacturer's protocol. The expression levels of *sek-1, daf-16, lys-7,* and *sma-3* were quantified by means of qPCR. In order to accurately determine relative expression levels, housekeeping genes *act-1, rps-23,* and *rpb*-12 served as internal controls. Primers were made *de novo*, adapted from Kwon et al. (2016) [76], or kindly provided by Luca Golinelli. A comprehensive list of all primers can be found in Table S1. The qPCR assays were conducted using the StepOnePlus™ System (ThermoFisher Scientific) in combination with the Power SYBR™ green qPCR master mix (ThermoFisher Scientific). Relative gene expression levels were determined by employing the ΔΔCt method, with non-infected worms as the control condition [75].

4.7. hilA gene expression measurement

A transcriptional *gfp*mut3-promoter fusion plasmid was electroporated into wild-type and Δ*csgD* strains genomically labelled with mRFP1 [77]. Nematodes were infected with these transformed strains and at different time points post-infection, around 100 nematodes were pooled, washed, and lysed as described above.

Flow cytometric analysis was conducted using the CytoFLEX S (Beckman Coulter). Non-infected worms and bacteria either lacking the promoter-fusion or constituently expressing *gfp*mut3 were used to optimize the acquisition settings. Fluorescence, forward, and side scatter data were collected for at least 1000 *Salmonella* cells, as determined via gating based on size and red fluorescence. Data analysis was carried out using the FlowJo software.

4.8. Confocal microscopy

Δ*sek-1(km4)* mutant worms were infected as described above. For confocal imaging, the worms were mounted with 25 mM sodium azide on 2 % agarose pads on a glass slide and covered with a cover slide. Bacterial colonization was observed using a LSM 880 confocal laser scanning microscope (Carl Zeiss NV) combined with an Airyscan Detector using the 63× (oil immersion) objective and the associated Zen Blue software. 488 nm and 510 nm lasers were used for visualization of *gfpmut3* and *dsRed,* respectively. Confocal images were analyzed using the Zen Blue and Fiji software.

4.9. Statistical analysis

The survival assay data was analyzed and Kaplan-Meier survival plots were generated using the OASIS2 tool [78,79]. The colonization and immune assays were processed using mixed model analysis in R and graphical presentations were crafted using GraphPad Prism Software, version 8.4.3.

Funding

This work was supported by the KU Leuven Research Fund (C24/18/046), by Research Foundation Flanders (FWO) (W000921 N), and by FPS Public Health (RF 21/6343). I.T. and M.L. were funded by a doctoral fellowship from FWO (1S45924 N and 1S36020 N, respectively).

Declaration of Generative AI and AI-assisted technologies in the writing process

During the preparation of this work the author(s) used ChatGPT in order to proofread pieces of text. After using this tool/service, the author (s) reviewed and edited the content as needed and take(s) full responsibility for the content of the publication.

CRediT authorship contribution statement

Ines Thiers: Writing – review & editing, Writing – original draft, Methodology, Investigation, Formal analysis, Conceptualization. **Maries Lissens:** Methodology, Investigation, Conceptualization. **Hanne Langie:** Investigation, Formal analysis. **Bram Lories:** Writing – review & editing, Supervision, Resources, Project administration, Methodology, Funding acquisition, Conceptualization. **Hans Steenackers:** Writing – review & editing, Supervision, Resources, Project administration, Methodology, Funding acquisition, Conceptualization.

Declaration of competing interest

The authors declare the following financial interests/personal relationships which may be considered as potential competing interests:

Ines Thiers reports financial support was provided by Research Foundation Flanders. Maries Lissens reports financial support was provided by Research Foundation Flanders. Financial support was provided by Federal Public Service Public Health. If there are other authors, they declare that they have no known competing financial interests or personal relationships that could have appeared to influence the work reported in this paper.

Data availability

Data will be made available on request.

Acknowledgements

We are grateful to Liesbet Temmerman and Luca Golinelli for assistance in *C. elegance* maintenance and qPCR analysis; to Tom Belpaire for assistance in confocal microscopy; to Gitta De Wit for providing the genomically-labelled *Salmonella* strains; and to Bart Braeckman for providing the appropriate *C. elegans* strain.

Appendix A. Supplementary data

Supplementary data to this article can be found online at https://doi.org/10.1016/j.bioflm.2024.100225.

References

[1] Stanaway JD, Parisi A, Sarkar K, Blacker BF, Reiner RC, Hay SI, et al. The global burden of non-typhoidal salmonella invasive disease: a systematic analysis for the Global Burden of Disease Study 2017. Lancet Infect Dis 2019;19:1312–24. https://doi.org/10.1016/S1473-3099(19)30418-9.

[2] Winfield MD, Groisman EA. Role of nonhost environments in the lifestyles of *Salmonella* and *Escherichia coli*. Appl Environ Microbiol 2003;69:3687–94. https://doi.org/10.1128/AEM.69.7.3687-3694.2003.

[3] Steenackers H, Hermans K, Vanderleyden J, De Keersmaecker SCJ. *Salmonella* biofilms: an overview on occurrence, structure, regulation and eradication. Food Res Int 2012;45:502–31. https://doi.org/10.1016/j.foodres.2011.01.038.

[4] Giaouris E, Chorianopoulos N, Skandamis P, Nychas G-J. Attachment and biofilm formation by *Salmonella* in food processing environments. In: Mahmoud BSM, editor. *Salmonella* - a dangerous foodborne pathogen. Rijeka: InTech; 2012. p. 157–80.

[5] Peng D. Biofilm Formation of *Salmonella*. Microbial biofilms - importance and applications. 2016. p. 232–49.

[6] Miller AL, Pasternak JA, Medeiros NJ, Nicastro LK, Tursi SA, Hansen EG, et al. *In vivo* synthesis of bacterial amyloid curli contributes to joint inflammation during *S.* Typhimurium infection. PLoS Pathog 2020;16:1–22. https://doi.org/10.1371/journal.ppat.1008591.

[7] Miller AL, Nicastro LK, Bessho S, Grando K, White AP, Zhang Y, et al. Nitrate is an environmental cue in the gut for *Salmonella enterica* serovar typhimurium biofilm dispersal through curli repression and flagellum activation via cyclic-di-GMP signaling. mBio 2022;13. https://doi.org/10.1128/MBIO.02886-21.

[8] Costa J, Ahluwalia A. Advances and current challenges in intestinal *in vitro* model engineering: a digest. Front Bioeng Biotechnol 2019;7. https://doi.org/10.3389/fbioe.2019.00144.

[9] Hewes SA, Wilson RL, Estes MK, Shroyer NF, Blutt SE, Grande-Allen KJ. *In vitro* models of the small intestine: engineering challenges and engineering solutions. Tissue Eng Part B 2020;26:313–26. https://doi.org/10.1089/ten.teb.2019.0334.

[10] Verma S, Srikanth CV. Understanding the complexities of *Salmonella* – host crosstalk as revealed by *in vivo* model organisms. International Union of Biochemistry and Molecular Biology 2015;67:482–97. https://doi.org/10.1002/iub.1393.

[11] Irazoqui JE, Urbach JM, Ausubel FM. Evolution of host innate defence: insights from *Caenorhabditis elegans* and primitive invertebrates. Nat Rev Immunol 2010;10:47–58. https://doi.org/10.1038/nri2689.

[12] Labrousse A, Chauvet S, Couillault C, Kurz CL, Ewbank JJ. *Caenorhabditis elegans* is a model host for *Salmonella* Typhimurium. Curr Biol 2000;10:1543–5.

[13] Portal-Celhay C, Blaser MJ. Competition and resilience between founder and introduced bacteria in the *Caenorhabditis elegans* gut. Infect Immun 2012;80:1288–99. https://doi.org/10.1128/IAI.05522-11.

[14] Desai SK, Padmanabhan A, Harshe S, Zaidel-Bar R, Kenney LJ. *Salmonella* biofilms program innate immunity for persistence in *Caenorhabditis elegans*. Proc Natl Acad Sci U S A 2019;116:12462–7. https://doi.org/10.1073/pnas.1822018116.

[15] Pérez-Morales D, Banda MM, Chau NYE, Salgado H, Martínez-Flores I, Ibarra JA, et al. The transcriptional regulator SsrB is involved in a molecular switch controlling virulence lifestyles of *Salmonella*. PLoS Pathog 2017;13:1–27.

[16] Worley MJ, Ching KHL, Heffron F. *Salmonella* SsrB activates a global regulon of horizontally acquired genes. Mol Microbiol 2000;36:749–61. https://doi.org/10.1046/j.1365-2958.2000.01902.x.

[17] Desai SK, Winardhi RS, Periasamy S, Dykas MM, Jie Y, Kenney LJ. The horizontally-acquired response regulator SsrB drives a *Salmonella* lifestyle switch by relieving biofilm silencing. Elife 2016;5:1–23. https://doi.org/10.7554/eLife.10747.

[18] Furukawa S, Kuchma SL, O'Toole GA. Keeping their options open: acute versus persistent infections. J Bacteriol 2006;188:1211–7. https://doi.org/10.1128/JB.188.4.1211-1217.2006.

[19] Costerton JW, Stewart PS, Greenberg EP. Bacterial biofilms: a common cause of persistent infections. Science 1998;284:1318–22. 1979.

[20] Flemming HC, Wingender J, Szewzyk U, Steinberg P, Rice SA, Kjelleberg S. Biofilms: an emergent form of bacterial life. Nat Rev Microbiol 2016;14:563–75. https://doi.org/10.1038/nrmicro.2016.94.

[21] MacKenzie KD, Wang Y, Shivak DJ, Wong CS, Hoffman LJL, Lam S, et al. Bistable expression of CsgD in *Salmonella enterica* serovar typhimurium connects virulence to persistence. Infect Immun 2015;83:2312–26. https://doi.org/10.1128/IAI.00137-15.

[22] White AP, Weljie AM, Apel D, Zhang P, Shaykhutdinov R, Vogel HJ, et al. A global metabolic shift is linked to *Salmonella* multicellular development. PLoS One 2010;5. https://doi.org/10.1371/journal.pone.0011814.

[23] Tenor JL, McCormick BA, Ausubel FM, Aballay A. *Caenorhabditis elegans* -based screen identifies *Salmonella* virulence factors required for conserved host-pathogen interactions. Curr Biol 2004;14:1018–24. https://doi.org/10.1016/j.

[25] MacKenzie KD, Palmer MB, Köster WL, White AP. Examining the link between biofilm formation and the ability of pathogenic *Salmonella* strains to colonize multiple host species. Front Vet Sci 2017;4:1–19. https://doi.org/10.3389/fvets.2017.00138.

[27] Bajaj V, Hwang C, Lee CA. *hilA* is a novel *ompR/toxR* family member that activates the expression of *Salmonella typhimurium* invasion genes. Mol Microbiol 1995;18:715–27.

[28] Darwin KH, Miller VL. The putative invasion protein chaperone SicA acts together with InvF to activate the expression of *Salmonella typhimurium* virulence genes. Mol Microbiol 2000;35:949–60. https://doi.org/10.1046/j.1365-2958.2000.01772.x.

[29] Hautefort I, Proença MJ, Hinton JCD. Single-copy green fluorescent protein gene fusions allow accurate measurement of *Salmonella* gene expression in vitro and during infection of mammalian cells. Appl Environ Microbiol 2003;69:7480–91. https://doi.org/10.1128/AEM.69.12.7480-7491.2003.

[30] Lories B, Roberfroid S, Dieltjens L, Coster D De, Foster KR, Steenackers HP, et al. Biofilm bacteria use stress responses to detect and respond to competitors. Curr Biol 2020;30:1231–44. https://doi.org/10.1016/j.cub.2020.01.065.

[31] Sánchez-romero MA, Casadesús J. Contribution of SPI-1 bistability to *Salmonella enterica* cooperative virulence: insights from single cell analysis. Sci Rep 2018;8: 1–11. https://doi.org/10.1038/s41598-018-33137-z.

[32] House D, Bishop A, Parry C, Dougan G, Wain J. Typhoid fever: pathogenesis and disease. Curr Opin Infect Dis 2001;14:573–8.

[33] Chen L-M, Hobbie S, Galán JE. Requirement of CDC42 for *salmonella*-induced cytoskeletal and nuclear responses. Science 1996;274:2115–8. 1979.

[34] Patel JC, Galán JE. Differential activation and function of Rho GTPases during *Salmonella*-host cell interactions. JCB (J Cell Biol) 2006;175:453–63. https://doi.org/10.1083/jcb.200605144.

[35] Friebel A, Ilchmann H, Aepfelbacher M, Ehrbar K, Machleidt W, Hardt WD. SopE and SopE2 from Salmonella typhimurium activate different sets of RhoGTPases of the host cell. J Biol Chem 2001;276:34035–40. https://doi.org/10.1074/jbc.M100609200.

[36] Brena D, Bertran J, Porta-de-la-Riva M, Guillén Y, Cornes E, Kukhtar D, et al. Ancestral function of Inhibitors-of-kappaB regulates *Caenorhabditis elegans* development. Sci Rep 2020;10. https://doi.org/10.1038/s41598-020-73146-5.

[37] Troemel ER, Chu SW, Reinke V, Lee SS, Ausubel FM, Kim DH. p38 MAPK regulates expression of immune response genes and contributes to longevity in *C. elegans*. PLoS Genet 2006;2:1725–39. https://doi.org/10.1371/journal.pgen.0020183.

[38] Youngman MJ, Rogers ZN, Kim DH. A decline in p38 MAPK signaling underlies immunosenescence in *Caenorhabditis elegans*. PLoS Genet 2011;7. https://doi.org/10.1371/journal.pgen.1002082.

[39] Kamaladevi A, Balamurugan K. Role of PMK-1/p38 MAPK defense in *Caenorhabditis elegans* against *Klebsiella pneumoniae* infection during host-pathogen interaction. Pathog Dis 2015;73:1–9. https://doi.org/10.1093/femspd/ftv021.

[40] Aballay A, Drenkard E, Hilbun LR, Ausubel FM. *Caenorhabditis elegans* innate immune response triggered by *Salmonella enterica* requires intact LPS and is mediated by a MAPK signaling pathway. Curr Biol 2011;13:47–52. https://doi.org/10.1145/2087756.2087814.

[41] Kim DH, Feinbaum R, Alloing G, Emerson FE, Garsin DA, Inoue H, et al. A conserved p38 MAP kinase pathway in *Caenorhabditis elegans* innate immunity. Science 2002;297:623–6. 1979.

[42] JebaMercy G, Vigneshwari L, Balamurugan K. A MAP Kinase pathway in *Caenorhabditis elegans* is required for defense against infection by opportunistic *Proteus* species. Microb Infect 2013;15:550–68. https://doi.org/10.1016/j.micinf.2013.03.009.

[43] Ortiz A, Vega NM, Ratzke C, Gore J. Interspecies bacterial competition regulates community assembly in the *C. elegans* intestine. ISME J 2021;15:2131–45. https://doi.org/10.1038/s41396-021-00910-4.

[44] Portal-Celhay C, Bradley ER, Blaser MJ. Control of intestinal bacterial proliferation in regulation of lifespan in *Caenorhabditis elegans*. BMC Microbiol 2012;12. https://doi.org/10.1186/1471-2180-12-49.

[45] Gómez-Orte E, Cornes E, Zheleva A, Sáenz-Narciso B, De Toro M, Iñiguez M, et al. Effect of the diet type and temperature on the *C. elegans* transcriptome. Oncotarget 2018;9:9556–71.

[46] McColl G, Rogers AN, Alavez S, Hubbard AE, Melov S, Link CD, et al. Insulin-like signaling determines survival during stress via posttranscriptional mechanisms in *C. elegans*. Cell Metabol 2010;12:260–72. https://doi.org/10.1016/j.cmet.2010.08.004.

[47] Wolkow CA, Kimura KD, Lee M-S, Ruvkun G. Regulation of *C. elegans* life-span by insulinlike signaling in the nervous system. Science 1997;290:147–9. 1979.

[48] Murphy CT, Mccarroll SA, Bargmann CI, Fraser A, Kamath RS, Ahringer J, et al. Genes that act downstream of DAF-16 to influence the lifespan of *Caenorhabditis elegans*. Nature 2003;424.

[49] Battisti JM, Watson LA, Naung MT, Drobish AM, Voronina E, Minnick MF. Analysis of the *Caenorhabditis elegans* innate immune response to *Coxiella burnetii*. Innate Immun 2017;23:111–27. https://doi.org/10.1177/1753425916679255.

[50] Jia K, Thomas C, Akbar M, Sun Q, Adams-Huet B, Gilpin C, et al. Autophagy genes protect against *Salmonella typhimurium* infection and mediate insulin signaling-regulated pathogen resistance. Proc Natl Acad Sci U S A 2009;106:14564–9. https://doi.org/10.1073/pnas.0813319106.

[51] Zhou M, Liu X, Yu H, Yin X, Nie SP, Xie MY, et al. Cell signaling of *Caenorhabditis elegans* in response to enterotoxigenic *Escherichia coli* infection and *Lactobacillus zeae* protection. Front Immunol 2018;9:1–11. https://doi.org/10.3389/fimmu.2018.01745.

[52] Berg M, Monnin D, Cho J, Nelson L, Crits-Christoph A, Shapira M. TGFβ/BMP immune signaling affects abundance and function of *C. elegans* gut commensals. Nat Commun 2019;10. https://doi.org/10.1038/s41467-019-08379-8.

[53] Depraitère C, Darmon M. Growth of *Dictyostelium discoideum* on different species of bacteria. Ann Microbiol 1978;129 B:451–61.

[54] Holt JE, Houston A, Adams C, Edwards S, Kjellerup BV. Role of extracellular polymeric substances in polymicrobial biofilm infections of *Staphylococcus epidermidis* and *Candida albicans* modelled in the nematode *Caenorhabditis elegans*. Pathog Dis 2017;75. https://doi.org/10.1093/femspd/ftx052.

[55] Smolentseva O, Gu I, Gautier L, Sh I, Defrancesc AS, Losick R, et al. Mechanism of biofilm-mediated stress resistance and lifespan extension in *C. elegans*. Sci Rep 2017;7. https://doi.org/10.1038/s41598-017-07222-8.

[56] Aswathanarayan JB, Vittal RR. Inhibition of biofilm formation and quorum sensing mediated phenotypes by berberine in: *Pseudomonas aeruginosa* and *Salmonella* Typhimurium. RSC Adv 2018;8:36133–41. https://doi.org/10.1039/c8ra06413j.

[57] Donato V, Ayala FR, Cogliati S, Bauman C, Costa JG, Leñini C, et al. *Bacillus subtilis* biofilm extends *Caenorhabditis elegans* longevity through downregulation of the insulin-like signalling pathway. Nat Commun 2017;8. https://doi.org/10.1038/ncomms14332.

[58] Begun J, Gaiani JM, Rohde H, Mack D, Calderwood SB, Ausubel FM, et al. *Staphylococcal* biofilm exopolysaccharide protects against *Caenorhabditis elegans* immune defenses. PLoS Pathog 2007;3:526–40. https://doi.org/10.1371/journal.ppat.0030057.

[59] Tan M, Rahme LG, Sternberg JA, Tompkins RG, Ausubel FM. *Pseudomonas aeruginosa* killing of *Caenorhabditis elegans* used to identify. P. aeruginosa virulence factors 1999;96:2408–13.

[60] Dieltjens L, Appermans K, Lissens M, Lories B, Kim W, Van der Eycken EV, et al. Inhibiting bacterial cooperation is an evolutionarily robust anti-biofilm strategy. Nat Commun 2020;11:1–11. https://doi.org/10.1038/s41467-019-13660-x.

[61] Madsen JS, Lin YC, Squyres GR, Price-Whelan A, Torio A de S, Song A, et al. Facultative control of matrix production optimizes competitive fitness in *Pseudomonas aeruginosa* PA14 biofilm models. Appl Environ Microbiol 2015;81: 8414–26. https://doi.org/10.1128/AEM.02628-15.

[62] Tai J-SB, Mukherjee S, Nero T, Olson R, Tithof J, Nadell CD, et al. Social evolution of shared biofilm matrix components, 119. The Proceedings of the National Academy of Sciences; 2022. https://doi.org/10.1073/pnas.

[63] Dragoš A, Kiesewalter H, Martin M, Hsu CY, Hartmann R, Wechsler T, et al. Division of labor during biofilm matrix production. Curr Biol 2018;28:1903–1913.e5. https://doi.org/10.1016/j.cub.2018.04.046.

[64] Otto SB, Martin M, Schäfer D, Hartmann R, Drescher K, Brix S, et al. Privatization of biofilm matrix in structurally heterogeneous biofilms. mSystems 2020;5.

[65] Lissens M, Joos M, Lories B, Steenackers HP. Evolution-proof inhibitors of public good cooperation: a screening strategy inspired by social evolution theory. FEMS Microbiol Rev 2022;46. https://doi.org/10.1093/femsre/fuac019.

[66] Römling U, Bokranz W, Rabsch W, Zogaj X, Nimtz M, Tschäpe H. Occurrence and regulation of the multicellular morphotype in *Salmonella* serovars important in human disease. International Journal of Medical Microbiology 2003;293:273–85.

[67] Porta-de-la-Riva M, Fontrodona L, Villanueva A, Cerón J. Basic *Caenorhabditis elegans* methods: synchronization and observation. JoVE 2012. https://doi.org/10.3791/4019.

[68] Fields PI, Swanson RV, Haidaris CG, Heffron F. Mutants of Salmonella typhimurium that cannot survive within the macrophage are avirulent 1986;83.

[69] Porwollik S, Santiviago CA, Cheng P, Long F, Desai P, Fredlund J, et al. Defined single-gene and multi-gene deletion mutant collections in salmonella enterica sv typhimurium. PLoS One 2014;9. https://doi.org/10.1371/journal.pone.0099820.

[70] Davis RW, Botstein D, Roth JR. Advanced bacterial genetics: a manual for genetic engineering. New York: Cold Spring Harbor Laboratory of Quantitative Biology; 1980.

[71] Valdivia RH, Falkow S. Bacterial genetics by flow cytometry: rapid isolation of *Salmonella typhimurium* acid-inducible promoters by differential fluorescence induction. Mol Microbiol 1996;22:367–78.

[72] Kim J, Webb AM, Kershner JP, Blaskowski S, Copley SD. A versatile and highly efficient method for scarless genome editing in *Escherichia coli* and *Salmonella enterica*. BMC Biotechnol 2014;14. https://doi.org/10.1186/1472-6750-14-84.

[73] Recorbet G, Robert C, Givaudan A, Kudla B, Normand P, Faurie G. Conditional suicide system of *Escherichia coli* released into soil that uses the *Bacillus subtilis sacB* gene. Appl Environ Microbiol 1993:1361–6.

[74] Palominos MF, Calixto A. Quantification of bacteria residing in *Caenorhabditis elegans* intestine. Bio Protoc 2020;10. https://doi.org/10.21769/BioProtoc.3605.

[75] Powell JR, Ausubel FM. Models of *Caenorhabditis elegans* infection by bacterial and fungal pathogens. In: Ewbank J, Vivier E, editors. Methods in molecular biology. Totowa: Humana Press; 2008. p. 403–27.

[76] Kwon G, Lee J, Lim YH. Dairy *Propionibacterium* extends the mean lifespan of *Caenorhabditis elegans* via activation of the innate immune system. Sci Rep 2016;6. https://doi.org/10.1038/srep31713.

[77] Robijns SCA, Roberfroid S, Puyvelde S Van, Pauw B De, Uceda E, Weerdt A De, et al. A GFP promoter fusion library for the study of *Salmonella* biofilm formation and the mode of action of biofilm inhibitors. Biofouling 2014;30:605–25. https://doi.org/10.1080/08927014.2014.907401.

[78] Kaplan EL, Meier P. Nonparametric estimation from incomplete observations. J Am Stat Assoc 1958;53:457–81.

[79] Han SK, Lee D, Lee H, Kim D, Son HG, Yang J-S, et al. Oasis 2: online application for survival analysis 2 with features for the analysis of maximal lifespan and healthspan in aging research. Oncotarget 2016;7:56147–52.